ELSEVIER

Journal of Photochemistry and Photobiology A: Chemistry 123 (1999) 61–65

Journal of Photochemistry and Photobiology A:Chemistry

Excited state acidity of bifunctional compounds. 6. A novel, high fluorescence quantum yield, excited state intramolecular proton transfer compound: 2-hydroxyphenyl-lapazole in non-protic solvents[1]

Carlos E.M. Carvalho[a], Ira M. Brinn[a,*], Antonio V. Pinto[b], Maria C.F.R. Pinto[b]

[a]*LERT, Laboratório de Espectroscopia Resolvida no Tempo, Instituto de Química, Universidade Federal do Rio de Janeiro C.P. 68.563, Ilha do Fundão, Rio de Janeiro RJ, 21.941-970, Brazil*

[b]*NPPN, Núcleo de Pesquisa de Produtos Naturais, Universidade Federal do Rio de Janeiro, CP 68.563, Ilha do Fundão, Rio de Janeiro RJ, 21.941-970, Brazil*

Received 21 July 1998; accepted 26 January 1999

Abstract

The synthesis of 2-hydroxyphenyl-lapazole (HPL) is reported for the first time. HPL in the first excited singlet state undergoes excited state intramolecular proton transfer (ESIPT) in cyclohexane, with an overall fluorescence quantum yield of 0.15. This is an order of magnitude greater than that observed for 2-hydroxyphenyl-benzoxazole (HBO), which has been extensively studied and has a similar structure. At room temperature in non-protic solvents, ESIPT in HPL attains equilibrium, whose constant (between normal and tautomer species) is approximately 1.4. These observations suggest that HPL (and its derivatives) is well worth investigating because it is easier to study (and may work more efficiently as a laser dye) than HBO.

Keywords: ESIPT; High fluorescence quantum yield; Excited state equilibrium

1. Introduction

Recent developments in the field of ultrafast time-resolved fluorescence spectroscopy have led to considerable progress [2,3] in the study of excited state proton transfer (ESPT). The importance of ESPT is due to the fact that proton transfer is one of the few chemical reactions which is rapid enough to accompany the short-lived (normally, ns) first excited singlet state. Thus, as a theoretical tool, ESPT can be used as a probe [4] of excited singlet state electronic wave functions. It also has some potentially important applications, such as a fluorescence pH indicator which can be used at low concentrations because it is more sensitive than the usual absorption indicators, a lasing [5,6] material and the basis of a molecular size computer memory.

Given that the process of ESPT is important, a major question is which compounds can be used to study it. A compound which readily undergoes intramolecular ESPT (ESIPT) is 2-hydroxyphenyl-benzoxazole (HBO, Fig. 1) which, along with its derivatives, has been studied extensively. [7–12]. One serious disadvantage of this series of compounds is the generally low fluorescence quantum yields ($\Phi_{fl}=2\times10^{-2}$ for HBO [13], going below 10^{-3} for some of its derivatives). This problem can be attributed to efficient internal conversion, which has been discussed [14,15] within the concept of rotor size, the larger rotors being quenched less quickly. The present work introduces a rigid, bulky derivative of lapachone coupled to the oxazole moiety to produce 2-hydroxyphenyl-lapazole {9,9-dimethyl-2-(2′-hydroxyphenyl)-benzo[7,8]chromano[6,5-d][1,3]oxazole, HPL, Fig. 1.} In the following it is shown that HPL has various advantages over HBO.

2. Methods

HPL was synthesized by condensation [16] of β-lapachone with salicylaldehyde in the presence of ammonium acetate in glacial acetic acid. 1.27 g (16.5 mmol) of ammo-

*Corresponding author. Fax: +55-021-290-4746; e-mail: irabrinn@iq.ufrj.br

[1]Part 5. see [1].

1010-6030/99/$ – see front matter
PII: S1010-6030(99)00051-9

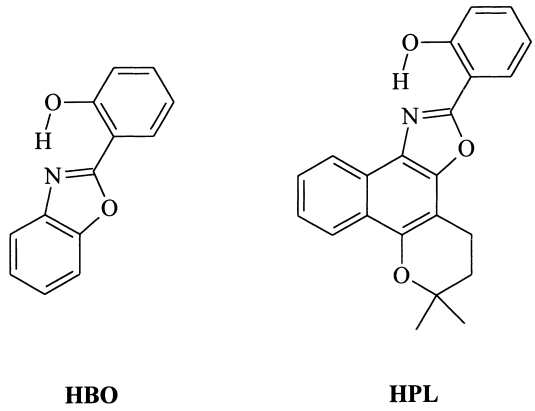

Fig. 1. 2-Hydroxyphenylbenzoxazole (HBO) and 2-hydroxyphenyl-lapazole (HPL).

nium acetate were added to a solution of β-lapachone (0.27 g, 1.1 mmol) and salicylaldehyde (0.31 g, 2.5 mmol) in 4 ml of acetic acid at 70°C and the reaction mixture was refluxed for 25 min. After cooling, the solution was added to 100 ml of water. The precipitate was filtered and washed thoroughly in water. The solid thus obtained was separated by column chromatography over silica gel, using a gradient mixture of *n*-hexane and ethyl acetate as eluent. HPL was found preferentially in the eluent fraction which was 27% (by volume) ethyl acetate. After drying, the product (0.17 g, 45%), white crystals of m.p.=205–207°C, was characterized by ^{1}H NMR (200 MHz $CDCl_3$) 11.60 (s, 1H), 8.30 (t, 2H), 7.98 (d, 1H), 7.50 (m, 3H), 7.20 (d, 1H), 7.00 (t, 1H), 3.20 (t, 2H), 1.98 (t, 2H), 1.23 δ (s, 6H); ^{13}C NMR (75 MHz $CDCl_3$) 160.1, 157.9, 148.0, 146.1, 132.0, 127.8, 126.8, 126.0, 124.2, 124.0, 123.9, 122.6, 121.8, 119.2, 117.0, 111.8, 101.8, 75.7, 31.8, 26.25, 17.75 ppm; IR (KBr) 2940, 2840, 1625, 1590, 1570, 1480, 1410, 1370, 1315, 1290, 1255, 1230, 1150, 1110, 1050,760, 735 720 cm^{-1}, MS *m/z* (%), $C_{22}H_{19}NO_3$ 345 (35), 302 (2,5), 289 (100), 169 (43,7), 121 (26,8); HRMS, calculated for $C_{22}H_{19}NO_3$: 345.136670, found: 345.136494. Its purity was verified by thin layer chromatography. All results agreed with the proposed structure.

Acetylation of HPL was done by adding 0.5 ml of dry pyridine to 20 mg (0.058 mmol) of HPL in acetic anhydride and heating at 60°C for 24 h. The reaction mixture was then evaporated under high vacuum and the residue recrystallized in *n*-hexane/acetone (9:1), yielding white needles of mp=129–131°C. ^{1}H NMR (200 MHz $CDCl_3$) 8.40 (d, 1H), 8.32 (dd, 1H), 8.30 (d, 1H), 7.60 (m, 1H), 7.50 (m, 2H), 7.40 (m, 1H), 7.20 (dd, 1H), 3.10 (t, 2H), 2.60 (s, 3H), 2.00 (t, 2H), 1.50 (s, 6H); MS *m/z* (%), $C_{24}H_{21}NO_4$ 387 (47), 345 (8.1), 331 (6.8), 289 (100), 169 (20.6), 121 (19.3); elem. anal.: calculated for $C_{24}H_{21}NO_4$: C, 74.39; H, 5.47; N, 3.61; O, 16.50; found: C, 75.26; H, 5.32; N, 3.20; O, 16.22.

Spectroquality grade methylcyclohexane (MCH, Aldrich) *n*-hexane and chloroform (Grupo Química) were used as received. Fluorescence quantum yield measurements were performed using a deaerated solution of 9,10-biphenyl anthracene in MCH as the standard [17].

The absorption spectra were taken on a Cary 1-E Spectrophotometer. The fluorescence spectra were obtained on a Hitachi F4500 Spectrophotofluorimeter, using Rhodamine B as an internal standard to generate corrected spectra. The time resolved measurements were done on the equivalent of an Edinburgh Instruments CD-900 time resolved spectrophotometer. The fluorescence lifetimes reported here were determined using the time resolved single photon counting method, utilizing a Hamamatsu R955 photomultiplier to measure emission. The excitation lamp was normally pulsed at 40 kHz and count rates did not exceed 1 kHz, to avoid pileup errors. Under these conditions, the equipment has a time resolution in the order of 200 ps. All lifetime values reported reflect data taken with at least 2×10^3 pulses in the maximum channel and a goodness of fit of $\chi^2\leq1.2$. A deaerated solution of anthracene in cyclohexane [17] was used as a time standard, with a monoexponential decay lifetime of 5.24 ns. The time profiles were analyzed using software based on the Marquardt [18] algorithm. The temperature variation studies were done using an Oxford Instruments Model no. DN1704 Liquid Nitrogen Cryostat.

3. Results

The absorption spectra of HPL show a structured $S_0\rightarrow S_1$ band in nonpolar solvents (Fig. 2). Its emission spectra (Fig. 2) exhibit two bands in every solvent tested. The blue band is structured and is the mirror image of the absorption

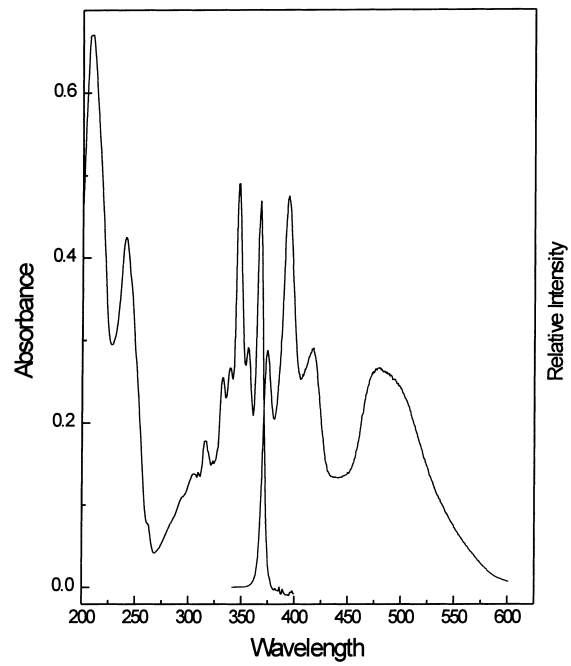

Fig. 2. Absorption and emission spectra of HPL (1×10^{-5} M) in *n*-hexane.

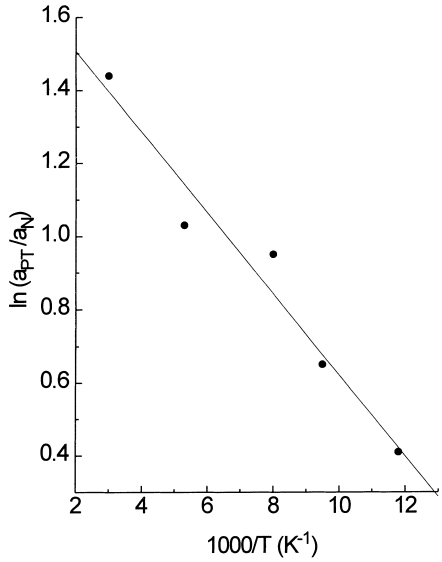

Fig. 3. Arrhenius plot of $\ln(a_{PT}/a_N)$ versus $1000/T$ for HPL in MCH. a_{PT} (λ_{em}=525 nm), a_N (λ_{em}=400 nm).

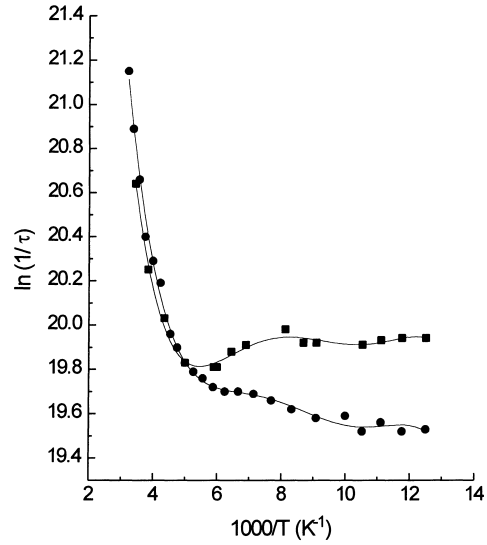

Fig. 4. Arrhenius plot of $\ln(1/\tau)$ versus $1000/T$ for HPL in MCH. (■) (λ_{em}=400 nm); (●) (λ_{em}=525 nm).

spectra, whereas the longer wavelength fluorescence band is neither and disappears upon acetylation. At ambient temperature no excitation wavelength dependence was observed for the relative integrated fluorescence intensities of the two bands (a_N/a_{PT}) in any solvent tested. At ambient temperature, the a_N/a_{PT} ratio is greater for HPL than for HBO in nonpolar solvents, typically being a factor of 0.25 for HPL and zero for HBO. The temperature dependence (between 80 and 300 K) of a_N/a_{PT} in MCH is shown in Fig. 3. The Arrhenius plot is quite linear in this range, with a slope of 1.1×10^2 K^{-1}. The overall (summed over both bands) fluorescence quantum yield is ϕ_{fl}=0.15±.05 at room temperature in cyclohexane, compared to ϕ_{fl}=0.90 for the standard [17].

The fluorescence decay times (Table 1) show monoexponential decay in acetonitrile, chloroform and MCH, varying between approximately 400 ps and 1.2 ns. The Arrhenius plots of the two decay constants of the emission bands at 400 and 525 nm in MCH are shown in Fig. 4. Both curves show obvious non-linear behavior, both bands having identical τ values at temperatures above 200 K and therefore the same E_a=13±1 kJ/mol. At lower temperatures, the bands have distinct τ values and the Arrhenius plots exhibit a second slope, with inclination close to zero.

Table 1
Experimental fluorescence lifetimes and quantum yields in various solvents at room temperature

Solvent	$\lambda_{exc}/\lambda_{em}$ (nm)	τ_1 (ns)	φ_{fl} [b]
Acetonitrile	317/375	0.44±.01[a]	
	336/500	0.40±.01	
Chloroform	331/400	1.23±.01	
	331/500	1.24±.01	
MCH	310/400	0.87±.01	0.15±.05
	310/500	0.84±.01	

[a] Most probable error.
[b] Standard: 9,10-biphenylanthracene in methylcyclohexane.

4. Discussion

The blue fluorescence band being the mirror image of the absorption spectrum indicates that the species emitting in this region resembles the ground state (N) structure. The fact that the green band is always structureless, independent of the solvent and that it disappears upon acetylation allows one to associate it with the proton transferred structure (PT). The presence of the green band, indicates that the strong hydrogen bond observed in the ^{1}H NMR spectra at δ=11.6 ppm (in $CDCl_3$) is not appreciably disrupted by the solvent.

In general, one would expect that different excited electronic states, having different electronic distributions, would exhibit different proton transfer rate constants. If also ESIPT in the higher excited singlet states, S_n (n>1), is rapid enough to compete with vibrational deactivation from $S_n \Rightarrow S_1$, the population distribution between the N and PT structures should be a function of the electronic state attained, which would imply that the relative intensities of the two fluorescence bands attributed to these two structures would vary with excitation wavelength (λ_{Exc}). However, in the solvents studied here, the a_N/a_{PT} ratio is observed to have no dependence on λ_{Exc}. This seems to imply that at least one of the above conditions does not hold. The first condition is so general that if it does not hold it would be purely coincidental and we will not consider this possibility any further. If the second condition did not hold, the S_1 state of the N species would form before appreciable proton transfer in S_n could take place. This would guarantee that the two species,

N and PT, would have the same excitation spectrum or, equivalently, that the relative intensity of the two fluorescence bands would be independent of λ_{Exc}. However, in this case, the system should have a biexponential decay kinetics, contrary to the single exponential which has been observed. Yet another possible explanation is that both ESIPT and reverse ESIPT in S_1 are rapid enough to compete efficiently with vibrational deactivation $S_1 \Rightarrow S_0$. In this case equilibrium between the two structures is attained during the lifetime of the first excited singlet state. This explanation is consistent with both the spectroscopic and kinetic results. (Note that the establishment of equilibrium in S_1 does not exclude the possibility that $k(S_n \Rightarrow S_1) \gg k$ (ESIPT in S_n).)

To the best of our knowledge, only two other systems have been reported to attain equilibrium while undergoing ESIPT, the double HBO [19,20] 2,5-*bis*-(2-benzoxazolyl)-hydroquinone (and its monomethylated derivative) in alkanes and 1-azacarbazole in ethanol, [21] albeit the latter is solvent assisted. The greater a_N/a_{PT} ratio in HPL, as compared to HBO, indicates a higher proton transfer quantum yield for HBO.

The temperature dependence of a_N/a_{PT} can be used to calculate the relative concentrations of each species in S_1 as follows;

$$K_{eq}(S_1) \equiv [PT^*]/[N^*] = (a_{PT}/a_N)\beta, \quad (1)$$

where β is the ratio of the fluorescence quantum yields of the two species times a correction factor for differences in instrumental sensitivity in the two wavelength regions. The latter factor can be neglected because all results reported here refer to corrected spectra. However,

$$\ln K_{eq}(S_1) = -\Delta G^0(S_1)/RT. \quad (2)$$

Therefore

$$\ln(a_{PT}/a_N) = -\Delta G^0(S_1)/RT - \ln\beta. \quad (3)$$

Assuming that β is independent of temperature, a plot of $\ln(a_{PT}/a_N)$ versus $1/T$ should generate a straight line whose slope is $\Delta G^0(S_1)/R$. The results in MCH are shown in Fig. 3, yielding $\Delta G^0(S_1) = -900 \pm 100$ J/mol. (The correlation coefficient, r was found to be 0.978, indicating that the supposition that β is temperature independent is reasonable.) Similar results [22] have been obtained for a double HBO in this temperature range. This generates $K_{eq}(S_1) = 1.44 \pm .06$, at 298 K. Assuming that the separation of the fluorescence maxima corresponds to the difference in the two 0-0 bands, one can calculate $\Delta G^0(S_0)$ by means of a pseudo Förster [23] cycle, yielding $\Delta G^0(S_0) = 70.3 \pm 0.3$ kJ/mol.

Knowing the overall fluorescence quantum yield, one can now calculate the fluorescence quantum efficiency (q_{PT}) of the species PT, considering

$$\phi_{fl} = \phi_N + \phi_{PT}, \quad (4)$$

where ϕ_{PT} is the apparent q_{PT}, needing to be corrected by the fraction of absorbed photons which leads to a PT species. This correction factor can be expressed as a function of $K_{eq}(S_1)$, being

$$q_{PT} = \phi_{PT}\{1 + 1/K_{eq}(S_1)\}. \quad (5)$$

The value of ϕ_N can be obtained in a straightforward manner, from the relative integrated fluorescence intensities below each curve, i.e.,

$$\phi_N = \{a_N/(a_N + a_{PT})\}\phi_{Fl}. \quad (6)$$

Eqs. (4)–(6) generate $q_{PT} = 0.20 \pm .07$ and $\phi_N = 0.03 \pm .01$, at 298 K.

The room temperature fluorescence decay results of HPL (Table 1) show that in acetonitrile, chloroform and MCH the kinetics are similar, i.e., the same monoexponential decay under both bands. It will be shown now that this result is also consistent with equilibrium being established during the lifetime of the excited singlet, by considering the following kinetic scheme

$$N \rightarrow N^* \quad I, \quad (7)$$

$$N^* \rightarrow N \quad k_N, \quad (8)$$

$$N^* \rightarrow PT^* \quad k_{PT,f}, \quad (9)$$

$$PT^* \rightarrow N^* \quad k_{PT,r}, \quad (10)$$

$$PT^* \rightarrow PT \quad k_T. \quad (11)$$

This kinetic scheme generates the differential equations

$$d[N^*]/dt = I[N] + k_{PT,r}[PT^*] - (k_N + k_{PT,f})[N^*], \quad (12)$$

$$d[PT^*]/dt = k_{PT,f}[N^*] - (k_T + k_{PT,r})[PT^*]. \quad (13)$$

The solution of differential equations (12) and (13) has been given [24–26], albeit for slightly different chemical systems, as the following biexponential decays

$$[N^*] = \{(k_T + k_{PT,r} - \lambda_1)\exp(-\lambda_1 t) + (\lambda_2 - k_T - k_{PT,r})\exp(-\lambda_2 t)\}/(\lambda_2 - \lambda_1), \quad (14)$$

$$[PT^*] = k_{PT,f}\{\exp(-\lambda_1 t) - \exp(-\lambda_2 t)\}/(\lambda_2 - \lambda_1), \quad (15)$$

where λ_1, λ_2 are the inverse of the experimentally determined decay times which satisfy [25] the relationships

$$\lambda_1 + \lambda_2 = k_N + k_T + k_{PT,f} + k_{PT,r}, \quad (16)$$

$$\lambda_1\lambda_2 = k_N(k_T + k_{PT,r}) + k_T k_{PT,f}. \quad (17)$$

If we consider the case in which the rate constants for proton exchange ($k_{PT,f}$ and $k_{PT,r}$) are considerably larger than the individual decay constants (k_N and k_T), we obtain the approximate results

$$\lambda_1 \cong k_{PT,f} + k_{PT,r}, \quad (18)$$

$$\lambda_2 \cong (k_N k_{PT,r} + k_T k_{PT,f})/(k_{PT,f} + k_{PT,r}). \quad (19)$$

(Considering the symmetry of Eqs. (16) and (17), λ_1 and λ_2 could be interchanged.) Consistent with the above assumptions, $\lambda_1 \gg \lambda_2$ and therefore $\exp(-\lambda_1 t) \ll \exp(-\lambda_2 t)$. Thus Eqs. (14) and (15) simplify to two monoexponen-

tials *with the same decay constant*, whose order of magnitude is the same as the individual decay constants

$$[N^*] \cong \exp(-\lambda_2 t)/(1 + k_{PT,f}/k_{PT,r}), \quad (20)$$

$$[PT^*] \cong \exp(-\lambda_2 t)/(1 + k_{PT,r}/k_{PT,f}). \quad (21)$$

This result is consistent with the experimental observation (Fig. 4) that equilibrium is attained only at higher temperatures (above 200 K) because only at higher temperatures will the condition be met that the proton exchange rate constants be considerably greater than the decay constants. This suggests that either the activation energies for the proton exchange processes are greater than the corresponding activation energies for decay (they were found [15] to be approximately equal for HBO and two derivatives), or else the reaction mechanism is different at lower temperatures.The ϕ_{fl} of 0.15 for HPL compares favorably with the value for HBO of 0.02. Considering that the latter represents only the PT form (only the green band is observed in the fluorescence spectrum of HBO), the value obtained here of ϕ_{PT}=0.20 is even more striking. From a knowledge of ϕ_{fl} and τ, one can calculate the radiative (k_{fl}) and nonradiative (k_{nr}) decay rate constant for each compound. For HBO at ambient temperature (in 3-methyl pentane) $k_{nr,HBO}=2.1\times10^9\ s^{-1}$ [15] and $k_{fl,HBO}=4.3\times10^7\ s^{-1}$. Using the experimental decay time in MCH (Table 1) and arbitrarily setting $\lambda_2 \cong k_T$ (a very rough approximation of Eq. (19)) one obtains $k_{nr,HPL}\cong 9.5\times10^8\ s^{-1}$ and $k_{fl,HPL}=2.4\times10^8\ s^{-1}$. A possible explanation for the difference in the radiative rate constants is that the coupling of the side rings on the benzo group (especially the aromatic ring), as one passes from HBO to HPL, causes the pi system to become more planar and rigid, increasing the overlap between the electronic wavefunctions of S_1 and S_0 and therefore increasing k_{fl}. It is worth mentioning that phenazines with the same benzochromano backbone as HPL have shown [27,28] the same general tendency of high absolute values of ϕ_{fl} and k_{fl}, in addition to higher k_{nr} in the case of the smaller molecular structures of the series relative to the larger phenazines.

5. Conclusions

HPL undergoes ESIPT and exhibits an overall fluorescence quantum yield which is considerably higher than the much studied HBO. Spectroscopic and time-resolved evidence presented here indicates that this new compound possesses unique photochemical properties and is worthwhile investigating further.

Acknowledgements

We gratefully acknowledge the Brazilian National Research Council (CNPq) for partial financial support (to CEMC and IMB), the World Bank and the Fund for Studies and Projects (FINEP) for an equipment grant and the José Bonifácio University Foundation (FUJB) for a maintenance grant.

References

[1] C. Carvalho, I. Brinn, W. Baumann, H. Reis, Z. Nagy, J. Chem. Soc., Faraday Trans. 93 (1997) 3325.
[2] L.G. Arnaut, S.J. Formosinho, J. Photochem. Photobiol. 75A (1993) 1.
[3] S.J. Formosinho, L.G. Arnaut, J. Photochem. Photobiol. 75A (1993) 21.
[4] N.S. Domingues, C. Krug, P.R. Livotto, V. Stefani, J. Chem. Soc., Perkin Trans. 2 (1997) 1861.
[5] C.V. Shank, A. Dienes, A.M. Trozzolo, J.A. Myer, Appl. Phys. Lett. 16 (1970) 405.
[6] A.M. Trozzolo, A. Dienes, C.V. Shank, J. Am. Chem. Soc. 96 (1974) 4699.
[7] R. Nakagaki, T. Kobayashi, S. Nagakura, Bull. Chem. Soc., Jpn. 51 (1978) 1671.
[8] G.J. Woolfe, M. Melzig, S. Schneider, F. Dörr, Chem. Phys. 77 (1983) 213.
[9] A. Mordzinski, A. Grabowska, W. Kuhnle, A. Krowczynski, Chem. Phys. Lett. 101 (1983) 291.
[10] B. Dick, Chem. Phys. Lett. 158 (1989) 37.
[11] P.-T. Chou, S.L. Studer, M. Martinez, Chem. Phys. Lett. 178 (1991) 393.
[12] M. Kasha, J. Heldt, D. Gormin, J. Phys. Chem. 99 (1995) 7281.
[13] A. Mordzinski, J. Lipkowski, G. Orzanowska, E. Tauer, Chem. Phys. 140 (1990) 167.
[14] M. Vogel, W. Rettig, Ber. Bunsenges. Phys. Chem. 91 (1987) 1241.
[15] A. Mordzinski, Excited State Intramolecular Proton Transfer: the Structural and Dynamic Aspects, Polish Academy of Science, Warsaw, 1990, p. 23.
[16] A.V. Pinto, C.V. Pinto, M.C.F.R. Pinto, R.S. Rita, C.A. Pezzella, S.L. de Castro, Arzneimittel-Forsch./Drug Res. 471 (1997) 74.
[17] D.F. Eaton, Pure Appl. Chem. 60 (1988) 1107.
[18] D.W. Marquardt, J. Soc. Ind. Appl. Math. 11 (1963) 431.
[19] A. Mordzinski, A. Grabowska, J. Mol. Struct. 114 (1984) 337.
[20] A. Grabowska, A. Mordzinski, N. Tamai, K. Yoshihara, Chem. Phys. Lett. 153 (1988) 389.
[21] J. Waluk, S.J. Komorowski, J. Herbich, J. Phys. Chem. 90 (1986) 3868.
[22] A. Mordzinski, A. Grabowska, K. Teuchner, Chem. Phys. Lett. 111 (1984) 383.
[23] T. Förster, Z. Elektrochem. 54 (1950) 42.
[24] K. Tsusumi, H. Shizuka, Z. Phys. Chem. (Wiesbaden) 122 (1980) 129.
[25] M. Hauser, Acta Phys. Chem. 30 (1984) 7.
[26] R. Krishnan, T.G. Fillingim, J. Lee, G.W. Robinson, J. Am. Chem. Soc. 112 (1990) 1353.
[27] A.V. Pinto, C.N. Pinto, M.C.F.R. Pinto, F.S. Emery, K.C.G. Moura, C.E.M. Carvalho, I.M. Brinn, Heterocyc. 45 (1997) 2431.
[28] C.E.M. Carvalho, I.M. Brinn, A.V. Pinto, M.C.F.R. Pinto, in preparation.